P H Y S I C A L   R E V I E W   L E T T E R S

Atom Michelson Interferometer on a Chip Using a Bose-Einstein Condensate

Ying-Ju Wang,[1] Dana Z. Anderson,[1] Victor M. Bright,[2] Eric A. Cornell,[1] Quentin Diot,[1] Tetsuo Kishimoto,[1,*]
Mara Prentiss,[3] R. A. Saravanan,[2] Stephen R. Segal,[1] and Saijun Wu[3]

[1]*Department of Physics, University of Colorado, and JILA, National Institute of Standards and Technology
and University of Colorado, Boulder, Colorado 80309-0440, USA*
[2]*Department of Mechanical Engineering, University of Colorado, Boulder, Colorado 80309-0427, USA*
[3]*Department of Physics, Harvard University, Cambridge, Massachusetts 02138, USA*
(Received 9 July 2004; published 11 March 2005)

An atom Michelson interferometer is implemented on an ''atom chip.'' The chip uses lithographically patterned conductors and external magnetic fields to produce and guide a Bose-Einstein condensate. Splitting, reflecting, and recombining of condensate atoms are achieved by a standing-wave light field having a wave vector aligned along the atom waveguide. A differential phase shift between the two arms of the interferometer is introduced by either a magnetic-field gradient or with an initial condensate velocity. Interference contrast is still observable at 20% with an atom propagation time of 10 ms.

Atom interferometry offers exquisite precision measurement capability, much like its photon-based counterpart. For example, the fundamental limit on the atom Sagnac gyroscope signal-to-noise ratio is a factor of 10^{11} greater than its optical counterpart, given comparable enclosed areas and particle flux. Unlike their photon counterparts, however, atoms can be sensitive to electric and magnetic fields. In this respect, atom interferometry may be suited to a substantially larger set of sensor applications, though by the same token, it is sensitive to a larger variety of detrimental noise sources. On balance, atom interferometry experiments have revealed promising and sometimes stunning measurement capabilities [1–5].

The so-called ''atom chips'' seek to implement atom-based devices on a small scale [6–10]. On a single substrate one can, for example, incorporate conductors, magnetic elements, and optical components to produce fields that confine, control, and manipulate atoms. On that same substrate one might also incorporate atom detection and signal conversion. Moreover, because the source of the fields can be close to the atoms, typically one can apply much larger forces, or use much less power to apply those forces, in comparison with free-space systems. Of interest here is the fact that the atom-chip approach provides substantial control over the geometry of an atom interferometer.

This work reports the demonstration of an on-chip atom Michelson interferometer employing a Bose-Einstein condensate (BEC). An intrawaveguide optical standing wave serves to split, reflect, and recombine the BEC. Some other attempts to implement a coherent beam splitter or recombiner on a chip have used current-induced magnetic fields, typically forming double potential wells that merge and then split apart either in space, in time, or in both. Atom-atom interactions due to high density in the waveguide can cause instabilities during the splitting or recombining process in such double-well potential [11] and also

reduce the phase coherence [12]. Various detrimental atom-surface and atom-wire interactions [13–16] have also stymied attempts to demonstrate on-chip interference. The combined optical and magnetic forces employed here have enabled a study of the coherence properties of matter waves confined to a microstructure.

We introduce a differential phase shift between the two arms of the interferometer that modulates the atom interference. This differential phase shift is introduced by a
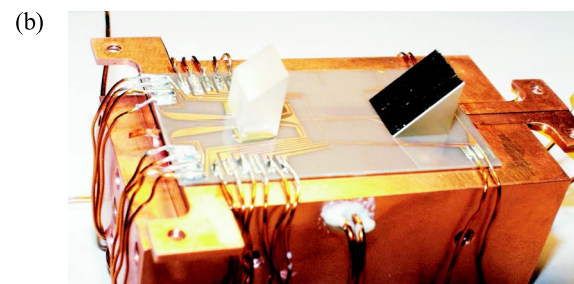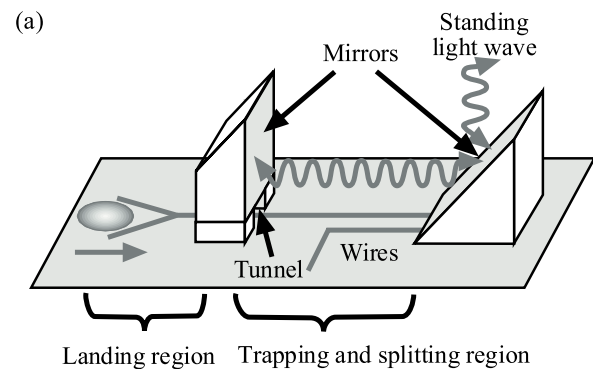

FIG. 1 (color online). (a) Schematic drawing of the atom chip (not to scale). The dimensions of the chip are 5 cm × 2 cm. (b) A photo image of the atom chip glued onto a copper holder.

magnetic-field gradient and alternatively by an initial condensate velocity in a trap with a longitudinal frequency of 5 Hz. We observe interference when the round-trip propagation time is relatively short, i.e., less than about 10 ms, and the maximum separation of the split wave packets is about 120 μm. The maximum separation is greater than the results reported previously for confined atom interferometers [17,18].

Our atom chip contains lithographically patterned wires and a pair of prism-shaped mirrors, as shown in Fig. 1. The wires generate magnetic fields that are essential for the microtrap and magnetic waveguide. The inward-facing surfaces of the two prisms are mirror coated to produce optical standing waves. A 180-μm-high tunnel is created underneath the prism located at the entrance side of the chip to allow for loading of the microtrap.

A cold cloud of ^{87}Rb is first collected in a magneto-optical trap. Atoms in the $|F = 1, m_f = -1\rangle$ state are loaded into a quadrupole trap produced by a pair of anti-Helmholtz coils. The coils are then mechanically moved to an adjoining chamber, and atoms are transferred into another magnetic trap with an Ioffe-Pritchard (IP) configuration. We apply rf-forced evaporative cooling until the cloud is around 0.45 μK, then the IP trap is turned off, and the cloud is pushed toward the chip in the third chamber by a magnetic gradient [19]. The cloud is delivered through the tunnel and captured in the chip's trapping region, which is located between the prisms and sits 115 μm away from the surface of the chip. After the cloud is loaded onto the chip, the trapping currents are reduced to place the cloud to 250 μm away from the surface. Next, rf-forced evaporative cooling is used again to form a condensate. The frequencies of the magnetic trap in which the condensate is made are 177 Hz in the radial and 10 Hz in the axial direction. Once a condensate is formed, the axial confinement is ramped down in 100 ms to release the condensate to the waveguide.

A tightly focused, linearly polarized laser beam with a waist of 110 μm is incident on and reflected by the mirror that is oriented at 45° with respect to the chip surface (see Fig. 1). The reflected beam is parallel to the surface of the chip and the direction of the waveguide. The beam is retroreflected by the second mirror that is perpendicular to the waveguide and the surface of the chip. The wave vector of the standing-wave light field needs to be parallel to the waveguide to minimize radial excitations of the BEC from photon scatterings. The prisms must be aligned with respect to the waveguide to better than 2°.

An interferometric measurement involves three standing-wave light pulses: a splitting pulse, a reflection pulse, and a recombining pulse. The frequency of the standing-wave light field is 7.8 GHz red detuned from the atomic resonance to minimize spontaneous emission. The condensate cloud begins at rest in the waveguide. The splitting pulse actually consists of a pair of subpulses,

and each subpulse diffracts atoms into different momentum states such as an optical diffraction grating in the Raman-Nath regime. The momentum of the atoms diffracted into the nth order is changed by $\pm 2n\hbar k$, where n is an integer number and k is the wave number of the photons [4,20].

In general, a single light pulse excites several different diffraction orders, which implies a coupling efficiency less than 100% into a particular order. To achieve a nearly ideal 50/50 splitting ratio, we have developed the double sub-pulse scheme [21]. The condensate starts at rest. Then the first pulse couples some of atoms into the $|p = \pm 2\hbar k\rangle$ state while the others stay in the $|p = 0\rangle$ state. The phase of atoms in the $|p = \pm 2\hbar k\rangle$ state evolves faster than that of the ones in the $|p = 0\rangle$ state. The differential phase shift can be written as $\Delta\phi = 4\omega_r\Delta t$, where $\omega_r = \hbar k^2/2m$ is the recoil frequency, m is the mass of atoms, and the Δt is the delay between the raising edges of the two pulses. Atoms in the different momentum states interfere as the second subpulse mixes them again. If the phase difference $\Delta\phi$ is a multiple of 2π, which corresponds to the delay $\Delta t = n\pi/2\omega_r$ between the two pulses, most atoms will populate in the $|p = \pm 2\hbar k\rangle$ state. On the other hand, if the phase difference is $(2n + 1)\pi$, which corresponds to the delay $\Delta t = (2n + 1)\pi/4\omega_r$, most atoms will remain in the zero momentum state after the double pulse. The contrast ratio of this interferometric splitting can be made 100% by optimizing the power and the length of the pulses [21]. In
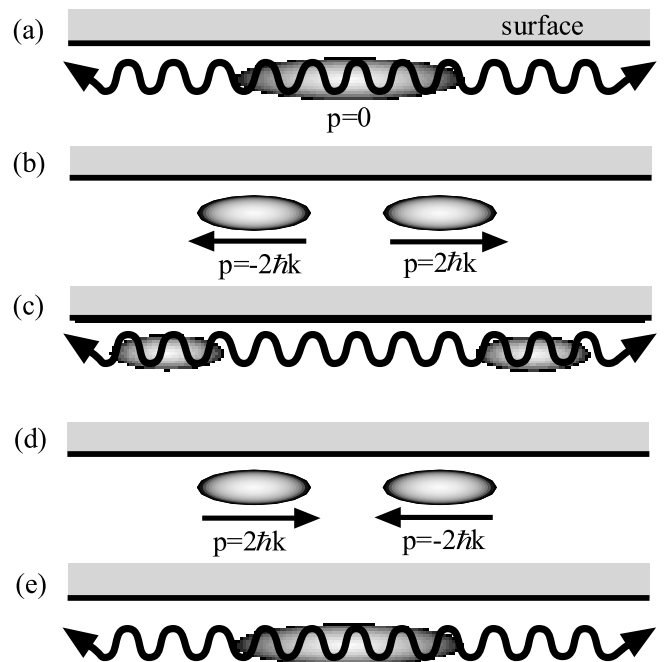

FIG. 2.   (a) The splitting pulse is turned on at $t = 0$. (b) The two split clouds propagate in the opposite direction at $0 < t < T/2$. (c) The reflection pulse is turned on at $t = T/2$. (d) The clouds propagate back toward to the center of the waveguide at $T/2 < t < T$. (e) The recombining pulse is turned on at $t = T$ when the clouds are overlapped.

our experiment, splitting of the atoms into the $|p = \pm 2\hbar k\rangle$ states, with nearly zero population in the $|p = 0\rangle$ or $|p = \pm 4\hbar k\rangle$ state, can be achieved; we find optimum splitting when the two pulses are both 20 μs in duration with power around 5.5 μW and the delay between the two pulses is 63 μs. The atoms in the different momentum states are detected by absorption imaging when the wave packets are spatially separated after 10 ms propagation.

A reflection pulse is used to reverse the direction of propagation of the two wave packets simultaneously. The pulse is chosen to be 150 μs in duration with power 6.2 μW. This relatively long pulse reverses the momenta of the wave packets through a Bragg scattering process [4,20]. In response to the reflection pulse, the clouds turn around and propagate back toward their origin.

Upon the return to their origin, a second pair of splitting pulses serves to recombine the two condensate clouds. The schematic drawings in Fig. 2 show the whole sequence of splitting, reflecting, and recombining the condensate atoms. Like a simple optical beam splitter or recombiner, our atom recombiner has two output ports. The first output port is represented by atoms having zero momentum, while the second port is represented by atoms having $|p| = 2\hbar k$. Because the splitting and recombining occur at the same spatial location, our atom interferometer is analogous to an optical Michelson interferometer. The relative phase shift between the two counterpropagating wave packets will change the fractional number of atoms in the two output ports. If the potential is perfectly symmetric, the relative phase shift should be zero, and the atoms should all be in the zero momentum state, as shown in Fig. 3(a). On the other hand, if the waveguide potential is not symmetric, the nonzero relative phase shift should lead to the presence of atoms in the $|p = \pm 2\hbar k\rangle$ state. In a special case where the relative phase shift is π, the number of atoms in the $|p = 0\rangle$ state should be nearly zero due to destructive interference, and all the atoms will appear in the $|p = \pm 2\hbar k\rangle$ state, as shown in Fig. 3(b). The populations in the two
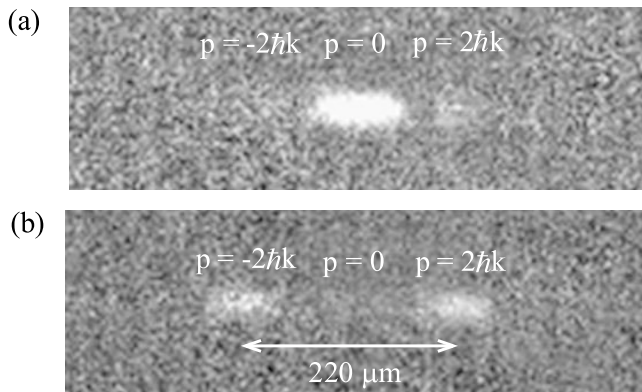
momentum states are anticorrelated since the total number is conserved.

To demonstrate interference, a differential phase shift is introduced by a magnetic gradient while the two wave packets are spatially separated after the splitting pulse. The differential phase shift $\Delta\phi_{\mathrm{mag}}$ can be written as

$$\Delta\phi_{\mathrm{mag}} = \int_{t1}^{t2} \frac{\Delta H}{\hbar} dt = \int_{t1}^{t2} \frac{\mu_{\mathrm{Rb}} B'(t)\Delta x(t)}{\hbar} dt, \quad (1)$$

where μ_{Rb} is the magnetic dipole moment of ^{87}Rb, B' is a time-dependent magnetic gradient, Δx is the time-dependent separation of the two clouds, t_1 is the time at which the magnetic gradient is turned on, and t_2 is the time at which the magnetic gradient is turned off. The differential phase shift arising from a time-varying magnetic field is referred to as the "scalar Aharonov-Bohm effect" in the inteferometry work by Shinohara $et\ al.$ [22]. The magnetic gradient is provided by a single wire that is perpendicular to the waveguide and 3.6 mm away from its center. The interference due to the change of the magnetic gradient is shown in Fig. 4. The total propagation time of condensates in the waveguide is 1 ms, and the time between each pulse is 0.5 ms. The magnetic gradient is switched on 0.25 ms before the reflection pulse for a duration of 0.5 ms. The maximum separation of the two clouds is around 12 μm, which is small compared to the full width at half maximum of the cloud size, ~100 μm. The contrast ratio shown in the figure is as large as 100%.

Interference is also observed after 10 ms propagation in the waveguide. An initial velocity of the condensate is created in the trap with a longitudinal frequency of 5 Hz. The two split clouds have different velocities after applying the splitting pulse because of the initial velocity. The clouds climb up the potential well to different heights and experience different potential during the total propagation
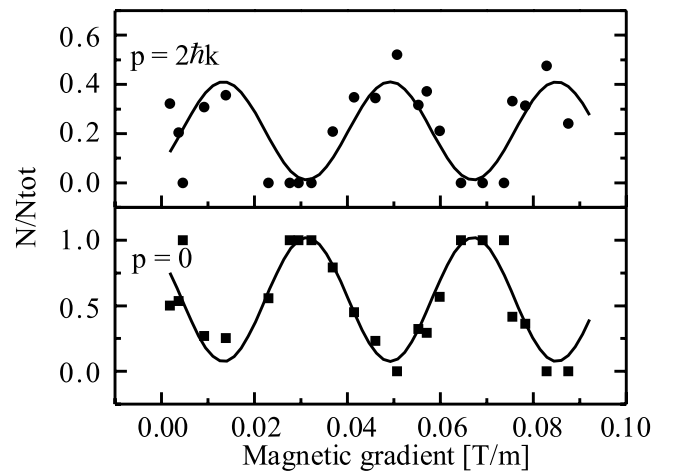
(a)

p = -2ħk   p = 0   p = 2ħk

(b)

p = -2ħk   p = 0   p = 2ħk

220 μm

FIG. 3. Interference pattern of (a) phase shift $= 2n\pi$ and (b) phase shift $= (2n + 1)\pi$. The absorption images are taken 10 ms after the recombining pulse.

FIG. 4. Interference fringes after 1 ms propagation time in the waveguide. The magnetic gradient is turned on for 500 μs and the average separation of clouds during the magnetic pulse is 8.82 μm.
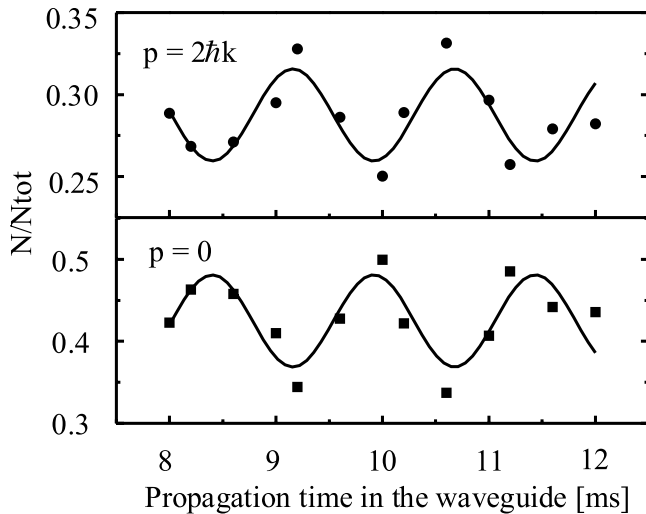
FIG. 5.   Interference fringes after about 10 ms propagation in the waveguide.

time, which is equivalent to an effective gradient. As a result, a differential phase shift accumulates as we increase the total propagation time. The interference is observed by changing the total propagation time in the waveguide, as shown in Fig. 5. The best contrast ratio of the interference at 10 ms, with maximum separation of the two clouds of about 120 μm, is 20%. The contrast ratio decreases rapidly as we increase the propagation time in the waveguide. We attribute this reduction of the contrast to the dispersion of the wave packets. The dispersion might arise from atom-atom interaction, an inhomogeneous guiding potential, or a nonzero curvature of the applied magnetic gradient; this topic requires further study.

In conclusion, we have demonstrated an on-chip atom Michelson interferometer. This is the first on-chip observation of atom interference between external states. The coherence of the wave packets has been observed up to 10 ms in the waveguide with a corresponding contrast ratio of 20%. The optical technique for splitting, reflecting, and recombining the condensates enables us to study decoherence effects that may affect coherent atom-chip devices in general.

*Present address: PRESTO, Japan Science and Technology Agency (JST), and Department of Applied Physics, School of Engineering, The University of Tokyo, Hongo 7-3-1, Bunkyo-ku, Tokyo 113-8656, Japan.
 [1] O. Carnal and J. Mlynek, Phys. Rev. Lett. **66**, 2689 (1991).
 [2] D. W. Keith *et al.*, Phys. Rev. Lett. **66**, 2693 (1991).
 [3] M. Kasevich and S. Chu, Phys. Rev. Lett. **67**, 181 (1991).
 [4] J. E. Simsarian *et al.*, Phys. Rev. Lett. **85**, 2040 (2000).
 [5] Y. Torii *et al.*, Phys. Rev. A **61**, 041602 (2000).
 [6] S. Schneider *et al.*, Phys. Rev. A **67**, 023612 (2003).
 [7] H. Ott *et al.*, Phys. Rev. Lett. **87**, 230401 (2001).
 [8] W. Hänsel *et al.*, Nature (London) **413**, 498 (2001).
 [9] M. Vengalattore, W. Rooijakkers, and M. Prentiss, Phys. Rev. A **66**, 053403 (2002).
[10] S. Wu, W. Rooijakkers, P. Striehl, and M. Prentiss, Phys. Rev. A **70**, 013409 (2004).
[11] J. A. Stickney and A. A. Zozulya, Phys. Rev. A **66**, 053601 (2002).
[12] S. Chen and R. Egger, Phys. Rev. A **68**, 063605 (2003).
[13] M. P. A. Jones *et al.*, Phys. Rev. Lett. **91**, 080401 (2003).
[14] A. E. Leanhardt *et al.*, Phys. Rev. Lett. **90**, 100404 (2003).
[15] J. Fortágh *et al.*, Phys. Rev. A **66**, 041604 (2002).
[16] A. E. Leanhardt *et al.*, Phys. Rev. Lett. **89**, 040401 (2002).
[17] D. S. Hall *et al.*, Phys. Rev. Lett. **81**, 1543 (1998).
[18] Y. Shin *et al.*, Phys. Rev. Lett. **92**, 050405 (2004).
[19] P. D. D. Schwindt, Ph.D. thesis, University of Colorado at Boulder, 2003 (http://jilawww.colorado.edu/bec/Publications/Thesis_Schwindt.pdf).
[20] P. J. Martin *et al.*, Phys. Rev. Lett. **60**, 515 (1988).
[21] S. Wu *et al.*, physics/0408011.
[22] K. Shinohara, T. Aoki, and A. Morinaga, Phys. Rev. A **66**, 042106 (2002).